Available online at www.sciencedirect.com
ScienceDirect
Ceramics International 37 (2011) 1761–1768
CERAMICS INTERNATIONAL
www.elsevier.com/locate/ceramint

Characterization and properties of microarc oxidized coatings containing Si, Ca and Na on titanium

Su cheng, Daqing Wei *, Yu Zhou, Haifeng Guo

Institute for Advanced Ceramics, Department of Materials Science and Engineering, Harbin Institute of Technology, Harbin 150001, PR China

Received 30 November 2010; received in revised form 20 December 2010; accepted 26 January 2011
Available online 9 March 2011

Abstract

To form bioactive microarc oxidized (MAO) coatings on titanium, the exploration for introducing various elements into the TiO_2-based MAO coatings has been continually noticed. In this work, novel MAO coatings containing Si, Ca and Na (SCN) elements were prepared on titanium. The elemental composition, mechanical properties, corrosion resistance and apatite-forming ability of TiO_2-based MAO coatings containing SCN were investigated. The surface hardness, elastic modulus, elastic recovery and corrosion resistance of the MAO coatings containing SCN were improved obviously by increasing the applied voltages. And the effect of applied voltage on the wetting ability of MAO coatings containing SCN is not significant. The current results indicated that the MAO coating containing SCN possesses good apatite-forming ability. The apatite-bonding structure is highly dependent on the chemical reactivity of the materials surface in simulated body fluid.

Keywords: C. Mechanical properties; D. Apatite; Corrosion resistance; Microarc oxidation; Titanium

1. Introduction

Microarc oxidation (MAO) is a relatively convenient and effective technique to deposit ceramic coatings on the surfaces of Ti, Al, Mg and their alloys [1]. This technique can introduce various desired elements into MAO coatings and produce various functional coatings with a porous structure [1]. Using MAO technique to deposit bioactive ceramic coatings on titanium and its alloys has received much attention in recent years [2–13]. According to the requirements of application environments, various MAO coatings containing different elements were fabricated by adjusting the electrolyte compositions. In most studies, Ca and P elements were introduced into MAO coatings for preparing the bioactive MAO coatings on Ti and its alloys. Thus various salts containing Ca and P such as calcium acetate, calcium glycerophosphate and calcium dihydrogen phosphate were used in MAO treatment process [2–13].

The exploration for introducing various elements into the MAO coatings to form bioactive surfaces has been continually noticed, such as only adding Ca or P, Sr [14–20]. As well known, silicon plays an important role in bone mineralization and formation and is therefore used in a wide variety of medical implants and bone grafts [21]. And most of the MAO coatings containing Si are used for engineering applications [1]. In this work, Si, Ca and Na (SCN) were doped into MAO coatings by using electrolytes containing sodium silicate, calcium acetate, EDTA-2Na and sodium hydroxide to form MAO coating on titanium for biomedical application, which has less been reported. This work reported the structure, mechanical properties, corrosion resistance and apatite-forming ability.

2. Experimental procedure

2.1. Sample preparation

In the MAO experiment, Ti plates ($10 \times 10 \times 1$ mm^3) were used as anodes and stainless steel plates were used as cathodes in an electrolytic bath. The plates were ground with 400, 800 and 1000# abrasive papers, washed with acetone and distilled water, and dried at 40 °C. An electrolyte was prepared by the dissolution of reagent-grade chemicals of $Ca(CH_3COO)_2{\cdot}H_2O$

* Corresponding author at: P.O. Box 3022#, Institute for Advanced Ceramics, Science Park, Harbin Institute of Technology, Yikuang Street, Harbin, 150080, PR China. Tel.: +86 451 8640 2040x8403; fax: +86 451 8641 4291.
E-mail address: daqingwei@hit.edu.cn (D. Wei).

0272-8842/$36.00
doi:10.1016/j.ceramint.2011.03.006

(8.8 g/l), Na_2SiO_3 (14.2 g/l), EDTA-2Na (15 g/l) and NaOH (20 g/l) into deionized water. The temperature of the electrolyte was kept at 40 °C by a cooling system. To investigate the effect of voltage on the structure and properties of the MAO coatings, the applied voltages of 200, 250, 300, 350, 400 and 450 V were used during the MAO treatment process. The frequency, duty cycle and oxidizing time were 600 Hz, 8.0% and 5 min.

2.2. Immersion of the samples in a simulated body fluid

The MAO coating formed at 300 V was soaked in 15 mL simulated body fluid (SBF) [22] (Table 1) immersing for different time and the SBF was refreshed every other day. The SBF was prepared by dissolving reagent-grade chemicals of NaCl, $NaHCO_3$, KCl, $K_2HPO_4{\cdot}3H_2O$, $MgCl_2{\cdot}6H_2O$, $CaCl_2$, and Na_2SO_4 into deionized water and buffering at pH 7.40 with tris-hydroxymethylaminomethane ($(CH_2OH)_3CNH_2$) and 1.0 mol/L HCl at 37 °C.

2.3. Test of mechanical and chemical properties

2.3.1. Wetting angle

Wetting angle of the MAO coatings was measured using the liquid drop method on a contact angle goniometer (CAM101, KSV Instruments Ltd, Finland).

2.3.2. Corrosion resistance

The corrosion resistance of the MAO coatings was investigated by a constant current potentiometer system (EG-G273, Shanghai Huachen, China) in SBF. In this system, the MAO samples were used as working electrode, and calomel and Pt were used as reference and assistant electrodes, respectively. The measured area of the MAO samples was 100 mm^2 and the scanning rate was set as 2 mv/s.

2.3.3. Nanoindentation test

A nanoindentation testing system (Nanoindenter XP, MTS, America) with a well-calibrated berkovich diamond indenter was employed to determine the mechanical properties. The maximum indentation depth and displacement resolution are 500 μm and 0.01 nm, respectively. The maximum load and load resolution are 500 mN and 50 nN, respectively. The change of temperature was kept below 1 °C and diamond tip drift limit was set at 0.25 nm/s. All continuous stiffness measurements were carried out under displacement control mode with tip-displacement rate of 10 nm/s. Load–displacement curves were recorded and elastic recovery was calculated. Hardness and elastic modulus were determined using the Oliver and Pharr method [23] for a constant depth of 1000 nm.

Table 1
Ion concentrations of the SBF and human blood plasma.

Ion	Concentrations (mmol/l)	
	SBF	Blood plasma
Na^+	142.0	142.0
K^+	5.0	5.0
Mg^{2+}	1.5	1.5
Ca^{2+}	2.5	2.5
Cl^-	147.8	103.8
HCO_3^{2-}	4.2	27
HPO_4^{2-}	1.0	1.0
SO_4^{2-}	0.5	0.5

2.3.4. Scratch test

Scratch test was performed to investigate the adhesion strength of MAO coatings on titanium. A constant load of 100 and 200 mN was applied on a diamond tip to draw a line on the coatings. The scratch surfaces were observed by a scanning electron microscopy (SEM).

2.4. Structure characterization

2.4.1. X-ray diffraction (XRD)

The phase composition of the sample surfaces were analyzed by X-ray diffraction (XRD, D/max-γB, Japan) using a CuKα radiation with a continuous scanning mode at a rate of 4°/min, under an accelerating voltage of 40 kV and current of 50 mA.

2.4.2. Scanning electron microscopy (SEM) and energy dispersive X-ray spectrometer (EDS)

A scanning electron microscopy (SEM, Quanta 200, FEI Co., American) was used to observe the surface morphologies of the MAO coatings after scratch test and SBF immersion. In addition, the elemental concentrations of the sample surfaces were detected by an energy dispersive X-ray spectrometer (EDS, EDAX, American) equipped on the SEM system.

2.4.3. X-ray photoelectron spectroscopy

An X-ray photoelectron spectroscopy (XPS, K-Alpha, Thermofisher Scientific Co., American) was used to detect the chemical compositions of the coating surfaces. In the XPS experiment, an AlKα (1486.6 eV) X-ray source was used for the XPS work under a vacuum of 1.0×10^{-8} mbar. The current of X-ray beam was 6 mA and the resolution for energy was 0.5 eV with a scanning step of 0.1 eV. The regions of 400 μm^2 on the sample surfaces were analyzed. The measured binding energies were calibrated by the C1s (hydrocarbon C–C, C–H) of 285 eV. And the chemical states of various elements before and after Ar^+ ions etching for 60 s were analyzed.

3. Results and discussion

3.1. Surface composition of the MAO coatings

The XPS survey results of the MAO coatings before and after Ar^+ ion etching is shown in Fig. 1. The major surface constituents observed on all the surfaces are Si, Ca, Ti, O, Na and C. Before etching, the C1 s peak was obviously higher compared to the etched samples due to the environmental contamination as shown in Fig. 1a. After etching, the Ca2p, Ti2p and Si2p peaks increased due to the removing of contaminated C as shown in Fig. 1b. The Ca2p and Si2p spectra of the MAO coatings are shown in Fig. 2. The Ca2p spectra reveal a doublet of $Ca2p_{3/2}$ at binding energy (BE) of 347.5 ± 0.2 eV and $Ca2p_{1/2}$ at BE of 351 ± 0.2 eV,

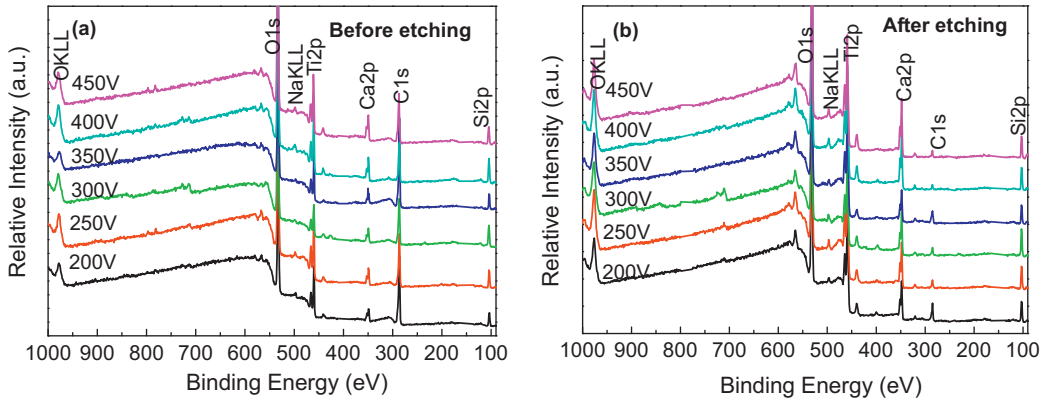

Fig. 1. XPS survey of the MAO coatings formed at different applied voltages before and after Ar^+ ions etching: (a) before etching and (b) after etching.

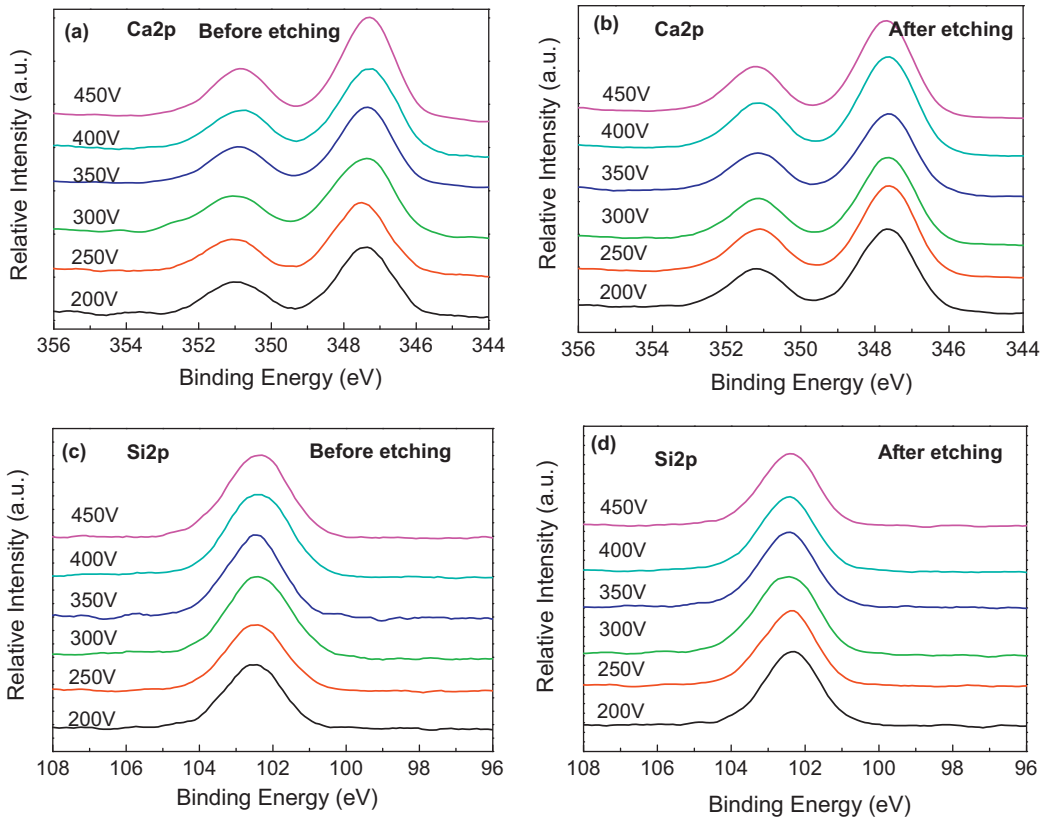

Fig. 2. XPS high-resolution spectra of Ca2p and Si2p of the MAO coatings formed at different applied voltages: (a) Ca2p and (b) Ca2p before and after etching, (c) Si2p and (d) Si2p before and after etching.

corresponding to Ca^{2+} [13]. The Si2p spectra reveal a peak at 102.5 ± 0.2 eV, corresponding to Si^{4+}. These results indicated that the applied voltage do not affect the chemical states of the Ca and Si. In addition, the XRD results indicated that the MAO coatings contained TiO_2 crystal and amorphous phase containing Si and Ca, et. [24].

3.2. Surface morphology and mechanical properties of the MAO coatings

Fig. 3 shows the SEM micrographs of the surfaces of titanium and MAO coatings after scratch test. After MAO treatment, porous coatings were formed on the titanium surface, and the pore size increased with increasing the applied voltage. Under a load of 100 mN, titanium surface shows a deep groove about 12 μm in width with a steep rim. Compared to titanium, the groove of the MAO coatings became shallow with increasing the applied voltage. The MAO coatings formed at 200 and 250 V show some cracks noted by white arrows in Fig. 3b and c. However, they also bonded with titanium substrate and did not be damaged completely. Under a load of 200 mN, except of the MAO coatings formed at 200 and 250 V, no cracks and scaling chips were found on other surfaces as shown in Fig. 4. Even, the pores were observed in the scratched regions of the MAO coatings formed at 400 and 450 V, showing a relatively slight scratch. The most of investigations on the

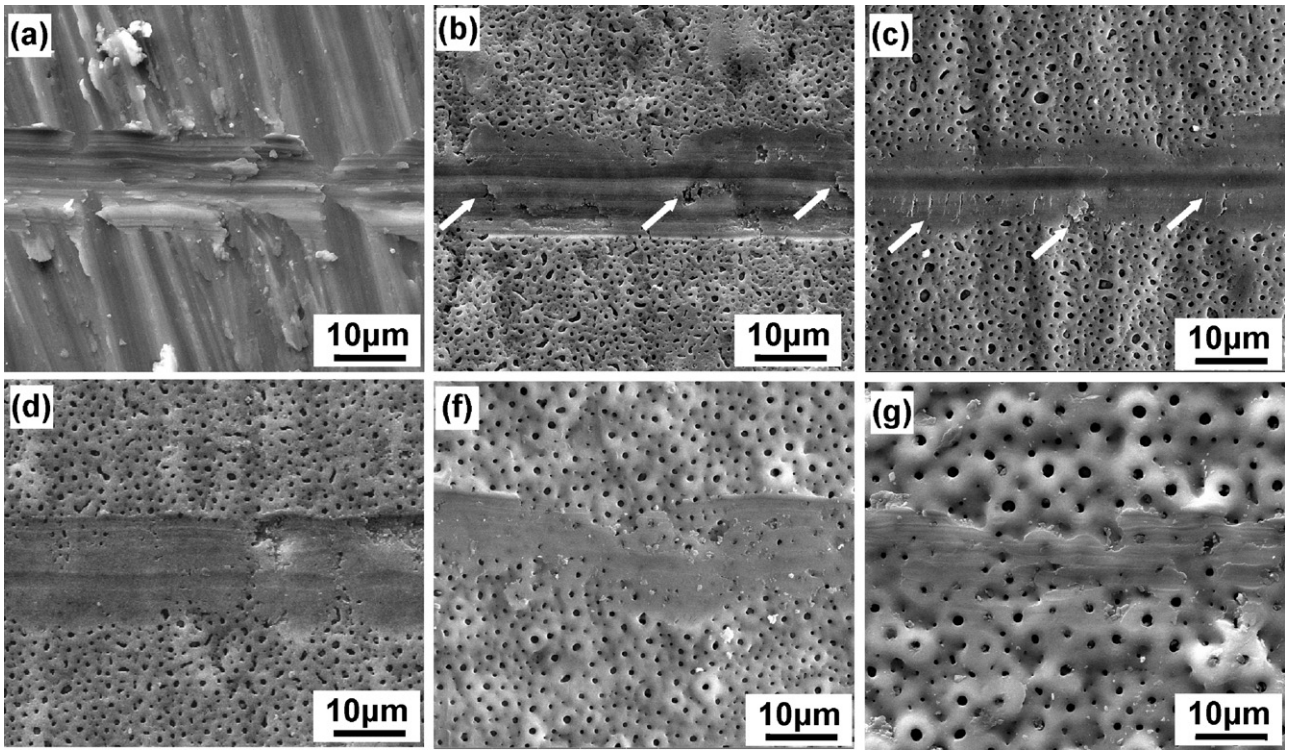

Fig. 3. SEM micrographs of the surfaces of titanium and MAO coatings formed at various voltages after scratch test with a load of 100 mN: (a) titanium, (b) 200 V, (c) 250 V, (d) 300 V, (e) 350 V, (f) 400 V and (g) 450 V.

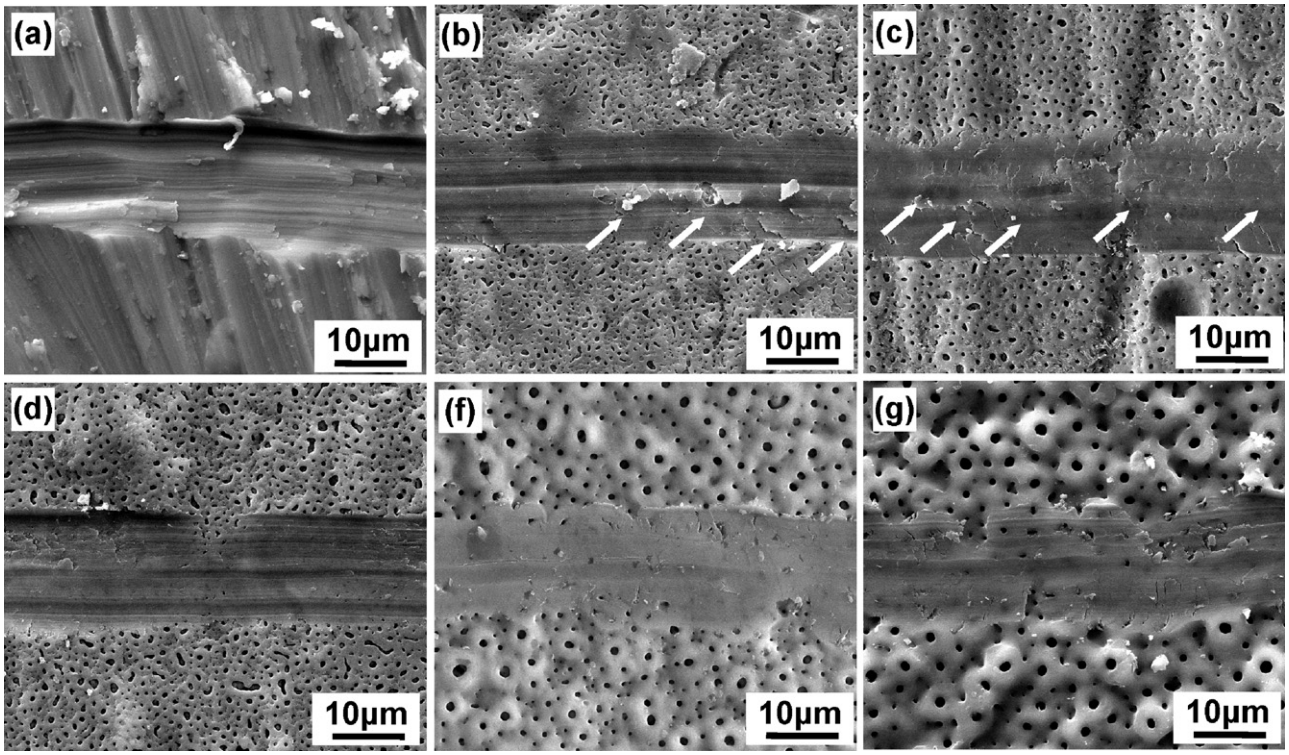

Fig. 4. SEM micrographs of the surfaces of the titanium and MAO coatings formed at various voltages after scratch test with a load of 200 mN: (a) titanium, (b) 200 V, (c) 250 V, (d) 300 V, (e) 350 V, (f) 400 V and (g) 450 V.

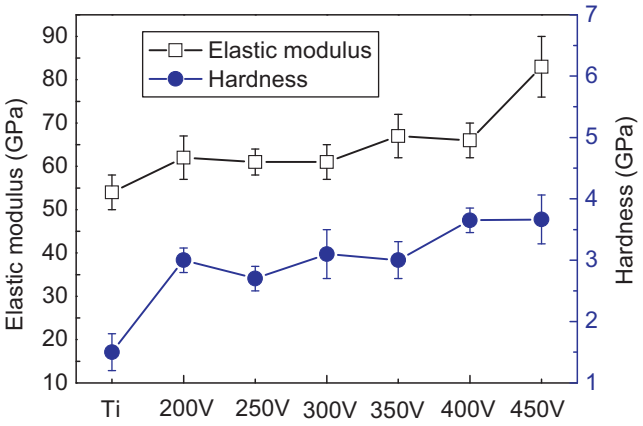

Fig. 5. The surface hardness and elastic modulus of titanium and MAO coatings formed at different applied voltages.

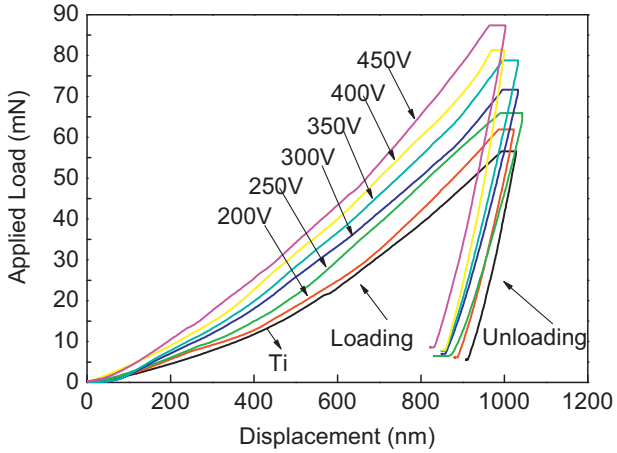

Fig. 6. Typical loading–displacement curves in an identical indentation depth of 1000 nm for the MAO coatings formed at different applied voltages.

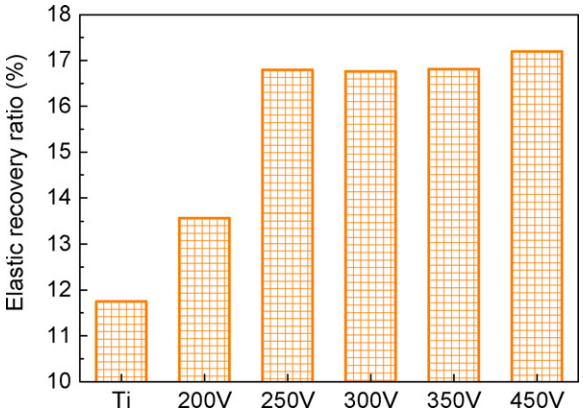

Fig. 7. The elastic recovery ratio for the MAO coatings formed at different applied voltages.

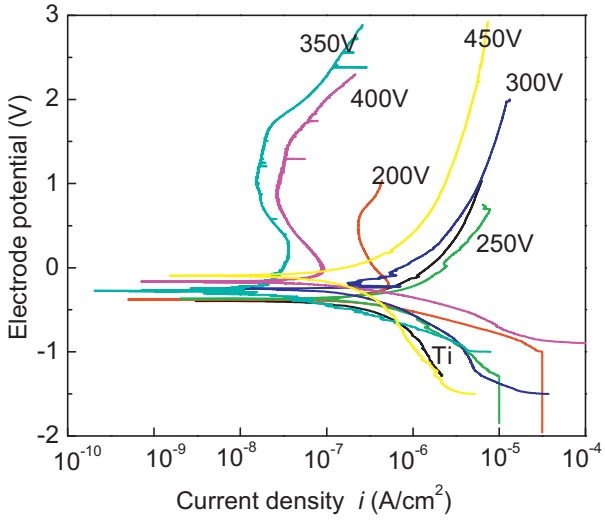

Fig. 8. The potentiodynamic polarization curves of titanium and MAO coatings formed at various voltages in the SBF.

bonding strength between MAO coatings and substrates, actually showed high bonding strength compared to other surface modification techniques such as sol–gel, etc. [25,26]. The results indicated that the increase of applied voltage could improve the mechanical strength of the MAO coatings, since the higher applied voltage promoted the formation of a large quantity of titania, as well as the incorporation of Si, Ca, etc.

Fig. 5 shows that the MAO coatings possess the higher hardness and elastic modulus compared to titanium. At the same time, the hardness and elastic modulus of the MAO coatings were improved as increasing the applied voltage. Fig. 6 shows the typical loading–displacement curves in an identical indentation depth of 1000 nm, and both loading and unloading curves are nonlinear. The maximum displacement achieved by the nanoindentation is originated from the elastic and plastic deformation during the testing process, and the elastic recovery is produced during the unloading duration. After MAO treatment of titanium surface, the maximum load performed on the surface when reaching the depth of 1000 nm was improved with increasing the applied voltages.

As shown in Fig. 7, the MAO coatings formed at various applied voltages showed higher elastic recovery compared to that of titanium. Generally, the residual displacement mainly depends on the plastic deformation. The ceramics basically exhibit low plastic deformation compared to metals, resulting in less residual displacement. Thus, the elastic recovery of titania ceramics is higher than that of titanium. Then, it was observed that the increasing applied voltages could increase the elastic recovery in the MAO coatings, as result of the formation of much titania at higher applied voltage.

3.3. Corrosion tests and wetting ability

The potentiodynamic polarization curves of titanium and MAO coatings in the SBF are plotted in Fig. 8. Compared to uncoated Ti, the MAO coatings show the high corrosion potential and lowest corrosion current. It was observed that increasing applied voltages could be favorable for improving corrosion resistance of the MAO coatings due to the increase of the MAO coating thickness and the formation of large quantity of titania. The MAO coatings should act as a barrier to the release of metal

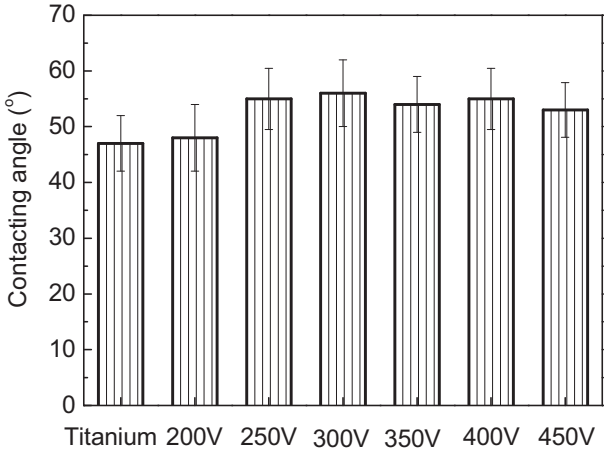

Fig. 9. Contacting angle of titanium and the MAO coatings formed at various voltages.

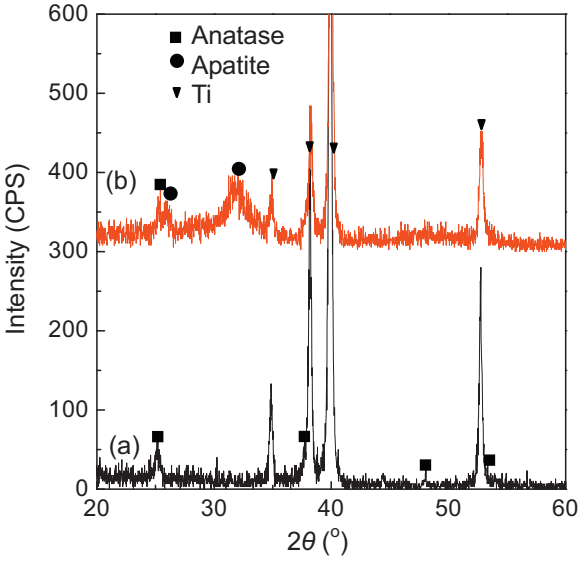

Fig. 10. XRD patterns of the MAO coatings prepared at 300 V before and after SBF immersion for 14 days: (a) before and (b) after immersion.

ions to human body and thus avoid deleterious effects. Fig. 9 shows the wetting angle of the titanium and MAO coating about the level of 46–55°. These results indicated that the applied voltage slightly affect the wetting ability of MAO coatings.

3.4. Apatite formation on the surface of the MAO coating

Fig. 10 shows the XRD patterns of the MAO coating formed at 300 V before and after SBF immersion for 2 weeks. It is evident that the surface of the MAO coating after SBF immersion show the apatite peaks, presenting apatite-forming ability. The surface morphologies of the MAO coating formed at 300 V after soaking in the SBF for 2, 3 and 4 weeks are shown in Fig. 11. Basically, a new apatite layer covered on the surface after SBF immersion for 2 weeks, except of local small region.

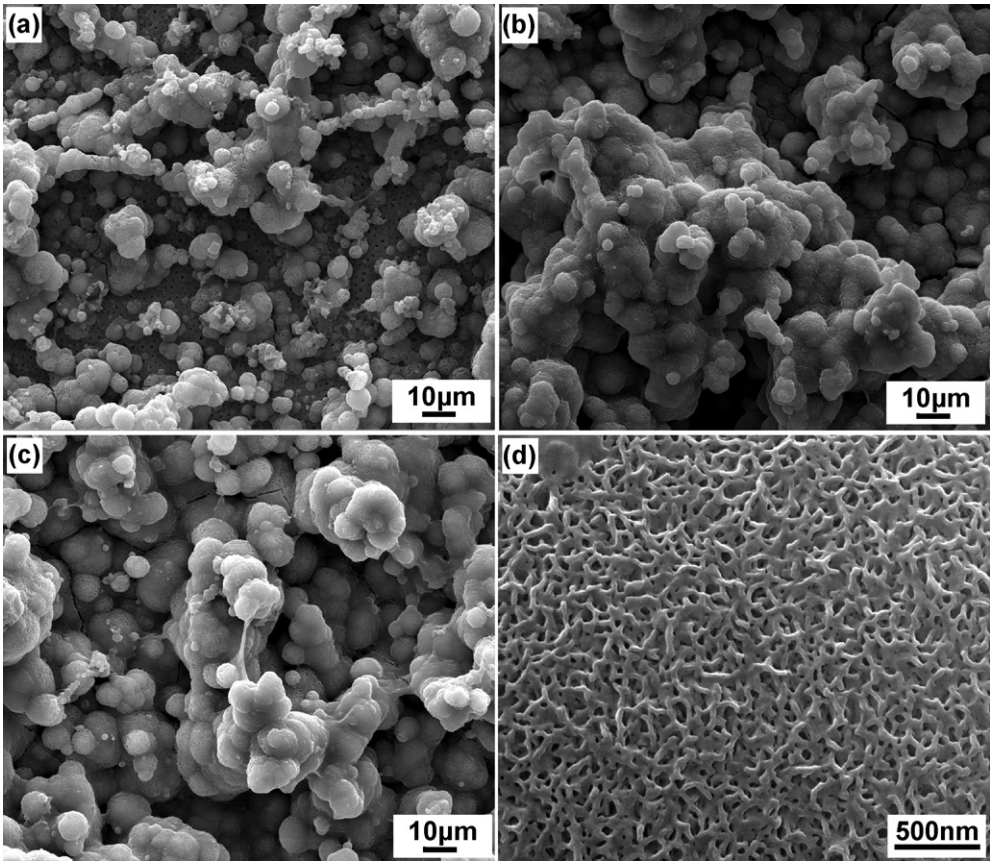

Fig. 11. SEM morphology of the MAO coating formed at 300 V after SBF immersion different periods: (a) 2 weeks, (b) 3 weeks, (c) 4 weeks and (d) high magnification of (c).

After immersion for 3 and 4 weeks, the apatite layer completely covered on the whole surface. The EDS result further indicated the Ca/P ratio is about 1.57 at 4 weeks. The Ca/P ratio of apatite is lower than that of HA. The apatite structure is very hospitable in allowing the substitutions of many other ions. The biomimetic apatite formed in SBF is similar to synthetic HA, but they differ from HA in composition, stoichiometry, and physical and mechanical properties. In fact, most investigations indicated that biomimetic apatites possess relative low Ca/P ratios due to the lack of Ca^{2+} ions in the apatite crystal, since the Ca^{2+} ions could be substituted by K^+, Na^+ and Mg^{2+} ions, and the PO_4^{3-} and OH^- groups could be substituted by HPO_4^{2-}, CO_3^{2-}, Cl^- and F^- ions.

The current results reveal that the MAO coating containing SCN has good induction capability for the heterogeneous nucleation and growth of apatite in the SBF. The applications of bioactive inorganic compounds containing Si, Ca, etc. such as bioactive glasses are very extensively, since they can bond to bone tissues well because it can induce a layer of biologically active hydroxycarbonate apatite spontaneously under a physiological environment due to the presence of Si, Ca, Na, etc. It is known that substrates with functionalized surfaces such as OH, PO_4H_2, COOH and $CONH_2$-terminated surfaces could induce the apatite formation in SBF or solutions containing various ions with respect to apatite [27].

The formation of apatite could be explained as following. Firstly, the deposition of apatite could be related with the formation of hydrated silica gel layer on the surfaces based on the previous researches [28], which could provide the chemical stimulus for the apatite deposition. The formation of hydrated silica gel is via dissolution of Na^+ ion from the surface based on the previous researches [28]:

$$Si(OSi)_3ONa + H_2O \rightarrow Si(OSi)_3OH + Na^+ + OH^- \quad (1)$$

$$Si(OSi)_3OH \rightarrow Si(OSi)_3O^- + H^+ \quad (2)$$

Moreover, the dissolution of Ca^{2+} ion into the SBF could also act as similar effect on the formation of OH group compared to Na^+ ion. At the same time, the dissolution of Ca^{2+} ion could further increase the local supersaturation near the surface of MAO coatings, promoting the deposition of calcium phosphates as shown in the following equation [28]:

$$Si(OSi)_3O^- + 2Ca^{2+} + P(V) \rightarrow Si(OSi)_3O^{d-}(Ca-O-PO_3-Ca)^{d+} \quad (3)$$

Generally, bonelike apatite formation on biomaterial surface in SBF requires a chemical stimulus. The apatite-bonding structure is highly dependent on the chemical reactivity of the materials surface in fluids.

4. Conclusion

The increase of applied voltages improved the surface hardness, elastic modulus and elastic recovery of the MAO coatings containing SCN. Increasing applied voltages could be favorable for improving corrosion resistance of the MAO coatings containing SCN due to the increase of the MAO coating thickness and the formation of large quantity of titania. The effect of applied voltage on the wetting ability of MAO coatings containing SCN is not significant. The SCN doped MAO coatings show good apatite-forming ability, which could be associated with the addition of SCN, involving various chemical reactivity of the materials surface in fluids, especially the formation of OH group.

Acknowledgements

This work was financially supported by National Natural Science Foundation of China (Grant Nos. 50872025 and 51002039), China Postdoctoral Science Foundation funded project and Heilongjiang province Postdoctoral Science Foundation funded project.

References

[1] A.L. Yerokhin, X. Nie, A. Leyland, A. Matthews, S.J. Dowey, Plasma electrolysis for surface engineering, Surf. Coat. Technol. 122 (1999) 73–93.
[2] D.Q. Wei, Y. Zhou, D.C. Jia, Y.M. Wang, Characteristic and in vitro bioactivity of microarc oxidized TiO_2-based coating after chemical treatment, Acta Biomater. 3 (2007) 817–827.
[3] D.Q. Wei, Y. Zhou, D.C. Jia, Y.M. Wang, Effect of heat treatment on the structure and in vitro bioactivity of microarc-oxidized (MAO) titania coatings containing Ca and P ions, Surf. Coat. Technol. 201 (2007) 8723–8729.
[4] D.Q. Wei, Y. Zhou, D.C. Jia, Y.M. Wang, Effect of applied voltage on the structure of microarc oxidized TiO_2-based bioceramic film, Mater. Chem. Phys. 104 (2007) 177–182.
[5] D.Q. Wei, Y. Zhou, Y.M. Wang, D.C. Jia, Characteristic of microarc oxidized coatings on titanium alloy formed in electrolytes containing chelate complex and nano-HA, Appl. Surf. Sci. 253 (2007) 5045–5050.
[6] D.Q. Wei, Y. Zhou, D.C. Jia, Y.M. Wang, Biomimetic apatite deposited on microarc oxidized anatase-based ceramic coating, Ceram. Int. 34 (2008) 1139–1144.
[7] M. Fini, A. Cigada, G. Rondelli, In vitro and in vivo behaviour of Ca- and P-enriched anodized titanium, Biomaterials 20 (1999) 1587–1594.
[8] X.L. Zhu, K.H. Kim, Y.S. Jeong, Anodic oxide films containing Ca and P of titanium biomaterial, Biomaterials 22 (2001) 2199–2206.
[9] X.L. Zhu, J.L. Ong, S.Y. Kim, K.H. Kim, Surface characteristics and structure of anodic oxide films containing Ca and P on a titanium implant material, J. Biomed. Mater. Res. 60 (2002) 333–338.
[10] Y. Han, S.H. Hong, K.W. Xu, Structure and in vitro bioactivity of titania-based films by micro-arc oxidation, Surf. Coat. Technol. 168 (2003) 249–258.
[11] V.M. Frauchiger, F. Schlottig, B. Gasser, M. Textor, Anodic plasma-chemical treatment of CP titanium surfaces for biomedical applications, Biomaterials 25 (2004) 593–606.
[12] L.H. Li, Y.M. Kong, H.W. Kim, Improved biological performance of Ti implants due to surface modification by micro-arc oxidation, Biomaterials 25 (2004) 2867–2875.
[13] W.H. Song, Y.K. Jun, Y. Han, S.H. Hong, Biomimetic apatite coatings on micro-arc oxidized titania, Biomaterials 25 (2004) 3341–3349.
[14] W.H. Song, H.S. Ryu, S.H. Hong, Apatite induction on Ca-containing titania formed by micro-arc oxidation, J. Am. Ceram. Soc. 88 (2005) 2642–2644.
[15] D.Q. Wei, Y. Zhou, Preparation, biomimetic apatite induction and osteoblast proliferation test of TiO2-based coatings containing P with a graded structure, Ceram. Int. 35 (2009) 2343–2350.

[16] K.C. Kung, T.M. Lee, T.S. Lui, Bioactivity and corrosion properties of novel coatings containing strontium by micro-arc oxidation, J. Alloy Compd. 2 (2010) 384–390.
[17] H.S. Ryu, W.H. Song, S.H. Hong, Biomimetic apatite induction of P-containing titania formed by micro-arc oxidation before and after hydrothermal treatment, Surf. Coat. Technol. 202 (2008) 1853–1858.
[18] Z.Q. Yao, Yu. Ivanisenko, T. Diemant, A. Caron, A. Chuvilin, J.Z. Jiang, R.Z. Valiev, M. Qi, H.J. Fecht, Synthesis and properties of hydroxyapatite-containing porous titania coating on ultrafine-grained titanium by micro-arc oxidation, Acta Biomater. 6 (2010) 2816–2825.
[19] Y. Han, D.H. Chen, J.F. Sun, Y.M. Zhang, K.W. Xu, UV-enhanced bioactivity and cell response of micro-arc oxidized titania coatings, Acta Biomater. 4 (2008) 1518–1529.
[20] J.Z. Chen, Y.L. Shi, L. Wang, F.Y. Yan, F.Q. Zhang, Preparation and properties of hydroxyapatite-containing titania coating by micro-arc oxidation, Mater. Lett. 60 (2006) 2538–2543.
[21] L.L. Hench, Bioceramics, J. Am. Ceram. Soc. 81 (1998) 1705–1728.
[22] A. Oyane, H.M. Kim, T. Furuya, T. Kokubo, T. Miyazaki, T. Nakamura, Biomimetic apatite coatings on micro-arc oxidized titania, J. Biomed. Mater. Res. A 65 (2003) 188–195.
[23] W.C. Oliver, G.M. Pharr, An improved technique for determining hardness and elastic-modulus using load and displacement sensing indentation experiments, J. Mater. Res. 7 (1992) 1564–1583.
[24] S. Cheng, D.Q. Wei, Y. Zhou, Structure of microarc oxidaized coatings containing Si, Ca and Na on titanium and deposition of cefazolin sodium/chitosan composite film, Surf. Coat. Technol., unpublished results.
[25] C.T. Wu, Y. Ramaswamy, D. Gale, W.R. Yang, K.Q. Xiao, L.C. Zhang, Y.B. Yin, H. Zreiqat, Novel sphene coatings on Ti–6Al–4V for orthopedic implants using sol–gel method, Acta Biomater. 4 (2008) 569–576.
[26] Y.M. Wang, L.X. Guo, J.H. Ouyang, Y. Zhou, D.C. Jia, Interface adhesion properties of functional coatings on titanium alloy formed by microarc oxidation method, Appl. Surf. Sci. 255 (2009) 6875–6880.
[27] G.K. Toworfe, R.J. Composto, I.M. Shapiro, P. Ducheyne, Nucleation and growth of calcium phosphate on amine-, carboxyl- and hydroxyl-silane self-assembled monolayers, Biomaterials 27 (2006) 631–642.
[28] S Hayakawa, K. Tsuru, C. Ohtsuki, A. Osaka, Mechanism of apatite formation on a sodium silicate class in a simulated body fluid, J. Am. Ceram. Soc. 82 (1999) 2155–2160.